Transport and Confinement Studies in RFX-mod Reversed-Field Pinch Experiment

P. Innocente, A. Alfier, L. Carraro, R. Lorenzini, R. Pasqualotto, M. Agostini, C. Alessi, V. Antoni, L. Apolloni, F. Auriemma, P. Bettini, T. Bolzonella, D. Bonfiglio, F. Bonomo, M. Brombin, A. Buffa, A. Canton, S. Cappello, R. Cavazzana, M. Cavinato, G. Chitarin, A. Cravotta, S. Dal Bello, A. De Lorenzi, L. De Pasqual, D.F. Escande, A. Fassina, P. Franz, G. Gadani, E. Gaio, L. Garzotti, E. Gazza, L. Giudicotti, F. Gnesotto, M. Gobbin, L. Grando, S.C. Guo, A. Luchetta, G. Malesani, G. Manduchi, G. Marchiori, D. Marcuzzi, L. Marrelli, P. Martin, S. Martini, E. Martines, A. Masiello, F. Milani, M. Moresco, A. Murari, L. Novello, S. Ortolani, R. Paccagnella, S. Peruzzo, R. Piovan, P. Piovesan, A. Pizzimenti, N. Pomaro, M.E. Puiatti, G. Rostagni, F. Sattin, P. Scarin, G. Serianni, P. Sonato, E. Spada, A. Soppelsa, G. Spizzo, M. Spolaore, C. Taccon, C. Taliercio, D. Terranova, V. Toigo, M. Valisa, N. Vianello, P. Zaccaria, P. Zanca, B. Zaniol, L. Zanotto, E. Zilli, G. Zollino, M. Zuin

Consorzio RFX, Euratom-ENEA Association, C.so Stati Uniti 4, I-35126, Padova, Italy

e-mail contact of main author: paolo.innocente@igi.cnr.it

Abstract. In RFX-mod external magnetic field coils and a close fitting thin conductive shell control radial magnetic fields. In the so-called Virtual Shell (VS) operation, radial field zeroing at the thin shell radius is stationary provided by the feedback-controlled coils. First experiments on RFX-mod proved the capability of the active scheme to steadily reduce the radial magnetic field. Furthermore it has been found that such edge magnetic field control extends its beneficial effects to the whole plasma. With respect to the old RFX, where MHD modes amplitude was controlled by the use of a passive thick conductive shell, a stationary 2 to 3-fold reduction of the B_r field amplitude in the core is obtained. The reduction of field fluctuations positively reflects on confinement. In fact, a strong reduction of the loop voltage is observed and correspondingly a 3-fold increase in pulse length is achieved by using the same poloidal flux swing. Temperature and particle measurements confirm the improved confinement properties of the virtual shell operation. With a lower ohmic input power, higher electron temperature in the plasma core and a steeper profile are measured. Particle and heat transport have been studied by means of a 1-D code. Local power balance was used to compute the heat conductivity profile: for the VS discharges a lower conductivity over a significant region of the plasma is found. The improved properties of RFX-mod VS operation provide a better confinement scaling both in terms of plasma current and density. The results show that compared to the thick shell configuration, a significant confinement improvement can be obtained under stationary conditions by actively controlling the plasma magnetic boundary.

1. Introduction

In reversed-field pinch (RFP) devices the magnetic configuration is characterized by a toroidal magnetic field whose direction at the plasma edge is opposite to that in the core. With an edge safety factor $q(a)=aB_t/RB_p \approx -0.02$, the toroidal magnetic field in the RFP is much smaller than in the Tokamak configuration and stability is ensured by a high magnetic shear ($r/q \cdot dq/dr$). In the RFP the safety factor is everywhere less than one, hence a large number of MHD modes are resonant and their amplitudes largely affect the confinement. In stationary conditions the RFP configuration is mainly sustained by internally self-generated plasma currents. Current self-generation is provided by the so-called dynamo mechanism. The magnetohydrodynamic (MHD) dynamo generates the required electric field by the nonlinear saturation of one or more resistive modes. While good magnetic surfaces could exist in a portion of the plasma edge [1], these dynamo modes produce field line stochasticity [2] that can affect confinement. On the other hand the RFP configuration allows copper toroidal coils, small size and large aspect ratio devices; furthermore RFPs do not need additional heating

systems. The open question about the RFP configuration is whether it will be possible to increase the energy confinement time towards values adequate for fusion reactors.
The MST experiment [3] has already transiently obtained Tokamak-like confinement, suppressing the dynamo mechanism by inductively driving the poloidal current. Experiments are underway aimed at finding a feasible method (NBI or RF current drive) to stationary drive a fraction of the poloidal current large enough to provide a good confinement.
The modified RFX experiment (RFX-mod) follows a different path [4,5]. In the so called 'Virtual Shell' (VS) operation mode, external feedback controlled magnetic field coils and a close fitting thin conductive shell cancel edge error fields and interact with the dynamo modes to reduce their amplitudes. The aim is to obtain good confinement conditions without the complication of additional current drive systems. Two conditions could help: the operation at high plasma current, at which lower amplitude dynamo modes are predicted [6], and the setting up of the 'quasi-single-helicity' (QSH) regime, in which one single dynamo mode much larger than the others provides most of the poloidal current. The QSH state resembles the 'single-helicity' state found in MHD computations [7] with which it shares the advantage of a lower stochasticity of the field lines [8].
In order to evaluate the feasibility of the RFX-mod approach, in this paper we study the global confinement properties and derive the transport parameters for a large database of discharges. To characterize the effect of the mode control, the RFX-mod VS results are directly compared with those obtained by the previous RFX thick shell operations and those obtained by RFX-mod operated without feedback control (NVS). The paper presents only stationary results although, like in the other RFPs, better confinement results are transiently possible in RFX-mod by inductively driving the poloidal current.
In sec. 2 the database of discharges is presented and confinement properties are discussed; in sec. 3 particle transport is analysed by means of a 1-d code; in sec. 4 energy transport is compared and the effect of QSH is presented.

2. Confinement

To study the confinement properties, a large database has been realised using all RFX and RFX-mod shots. To improve the analysis, kinetic quantities have been included in the database only if measured with small errors and profile measurements have been used where possible. Electron temperature profiles are computed by fitting Thomson Scattering multipoint measurements [9] by a two-parameter temperature profile $T_e(r)=T_{eo}(1-r^{\alpha})$. Electron density profiles are computed by inverting multi-chord interferometer measurements [10]. To account for hollow density profiles, we use a four parameters density profile $n_e(r)=n_{eo}-(n_{eo}-n_{e1}-n_{ea})r^{\alpha}-n_{e1}r^{\beta}$ [11]. Ion temperature was deduced by Doppler broadening of OVII lines when available.
Poloidal beta (β_p) (which in RFPs is about 50% higher than the volume average beta) and energy confinement time (τ_E) are computed by integrating temperature and electron density profiles. To increase the number of data-points the confinement analysis has been performed assuming $T_i=T_e$ because after the boronization procedure the OVII line emission is blended with Boron lines and the measurements of T_i

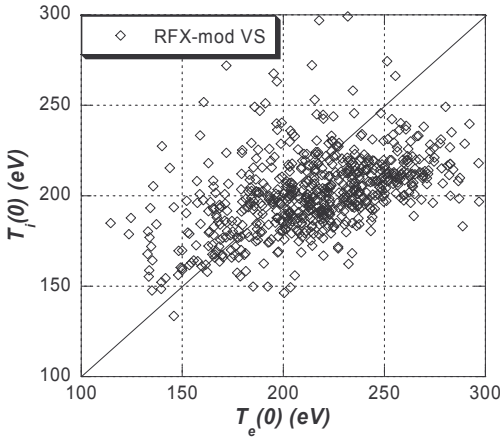

FIG. 1. Central ion temperature versus central electron temperature.

became very uncertain. The T_i=T_e assumption has been verified by comparing T_i with T_e, when both are available. Figure 1 shows that the two temperatures are approximately equal, with higher T_i at lower temperature and lower at higher temperature. The assumption T_i=T_e is hence justified at intermediate temperatures while it is conservative at low T. On the other hand, at high temperatures T_i measurements are affected from uncertainty in evaluating OVII radial position, which gives a systematic underestimation of T_i. The measurements of T_i with a neutral beam, recently installed on RFX-mod, will allow more precise evaluations in the near future.

The RFX experiments explored a large range in most of the operational parameters, with plasma current in the range I_p=0.1÷1 MA and density in the range n_e=0.5÷6·10^{19} m^{-3}. In FIG. 2 I_p/N ($N=\pi a^2<n>$ is the line density) and q(a) obtained at the different plasma currents I_p are shown for three RFX operation modes: RFX, RFX-mod NVS and RFX-mod VS. The figure shows that RFX-mod operates typically at a higher I_p/N parameter than the old RFX, in particular at currents over 800 kA the highest I_p/N are only obtained by RFX-mod. Finally, in RFX-mod currents over 600 kA are only explored with in VS mode to avoid first wall damage.

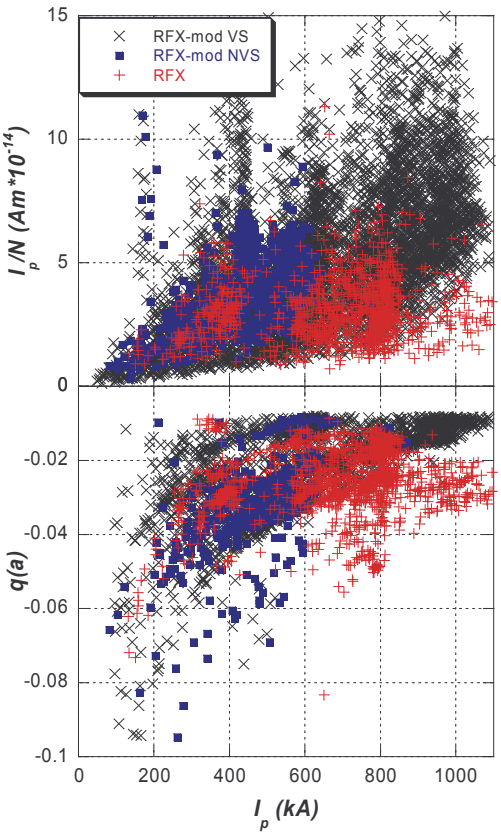

FIG. 2. Operational range in the (I,I/N) and (I_p,q(a)) parameters for RFX, RFX-mod standard operation (NVS) and RFX-mod with virtual shell (VS).

2.1 Confinement properties

The values of β_p and τ_E obtained for the three RFX experimental conditions are drawn in FIG. 3. Figure 3a shows that β_p varies from 2% to 15%, it is similar for both RFX-mod operation modes and is slightly higher than that of the thick shell RFX. Finally, it clearly

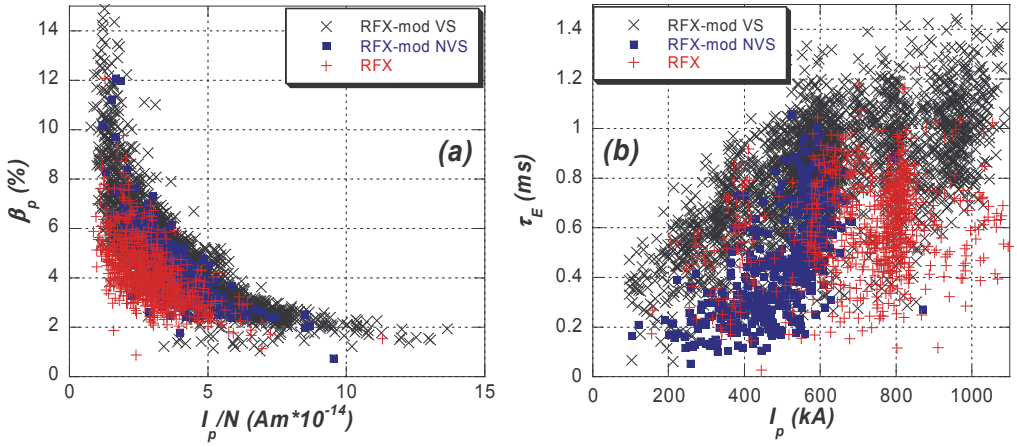

FIG. 3. Poloidal beta and energy confinement time for the three RFX experimental conditions.

depends on the I_p/N parameter. Figure 3b shows that τ_E can reach values up to 1.5 ms in RFX-mod, it is on average 50% higher for the VS operation compared to RFX and about twice than the RFX-mod NVS operation. Energy confinement time of RFX-mod steadily increases with plasma current while in RFX it showed a maximum at about 600÷800 kA.

A quantitative comparison of the performances in the three experimental conditions is obtained by averaging β_p and τ_E of stationary discharges (low dI_p/dt) in a small parameters range. Selecting the interval I_p=550÷600 kA, $I_p/N=3.5\div4.0\cdot10^{-14}$ Am and F=-0.25÷-0.05 ($F=B_t(a)/\langle B_t\rangle$) we obtained $\langle\beta_p\rangle$=3.4 %, $\langle\beta_p\rangle_{NVS}$=4 % and $\langle\beta_p\rangle_{VS}$=4.6 % for poloidal beta and $\langle\tau_E\rangle$=0.58 ms, $\langle\tau_E\rangle_{NVS}$=0.36 ms $\langle\tau_E\rangle_{VS}$=0.80 ms for energy confinement time. At higher currents, where only RFX and RFX-mod VS data are available, τ_E is two times higher for RFX-mod.

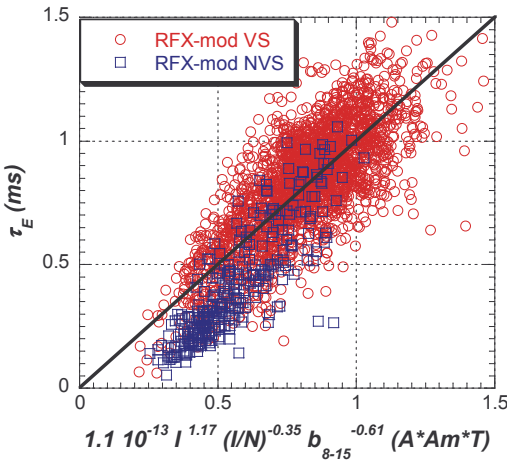

FIG. 4. Three parameters fit of τ_E of VS discharges applied to both VS and NVS RFX-mod discharges.

2.2 Scaling laws

To get some information about the phenomena underlying the confinement we study the dependences of β_p and τ_E on the main plasma parameters for RFX and RFX-mod VS.

Poloidal beta shows the strongest scaling and all the VS data of stationary discharges can be fitted by a single parameter exponential fit $\beta_p \propto (I_p/N)^{-0.74}$ (regression coefficient R=0.9). The RFX thick shell discharges are better described by a two parameters fit $\beta_p \propto I_p^{-0.46}(I_p/N)^{-0.50}$ (multiple regression coefficient R=0.7). The additional negative dependence on plasma current obtained in RFX is similar to that obtained in T2 experiment [12] and to the $\beta_p \propto I_p^{-0.56}(I_p/N)^{-0.56}$ predicted by 3-D resistive MHD simulations performed by DEBSP code. The result of RFX-mod VS shows that reducing plasma wall interaction by lowering edge error field is possible to obtain the same β_p at high plasma current.

Energy confinement time shows a less clear dependence on the main plasma parameters. In the RFX-mod VS case a two parameters fit provides the relatively good regression $\tau_E \propto I_p^{0.72}(I_p/N)^{-0.23}$ (multiple R=0.68) while a much worse (multiple R=0.3) regression $\tau_E \propto I_p^{0.40}(I_p/N)^{-0.16}$ is obtained in the RFX showing that other hidden parameters affect RFX results. A better scaling law is obtained for the VS data by a three parameters fit, using I_p, I_p/N and $b_{8\text{-}15}$, the sum of the amplitudes of the toroidal field modes with m=1 and n=-15÷-8. The least square fit of τ_E is drawn in figure 4. The goodness-of-fit has been tested by applying it to RFX-mod NVS data, for which $b_{8\text{-}15}$ is about 2÷3 times higher than for VS ones. Figure 4 shows that RFX-mod NVS data are also relatively well described. The explicit dependence of τ_E on b proves the beneficial effect of the boundary control up to the core. The dependence on b is qualitatively in accordance with the Rechester-Rosenbluth (RR) [2] theory of transport in a stochastic magnetic field, though numerical results [13] based on that theory would predict a power dependence of -1.5. It has to be noted that the best correlation was obtained using m=1 modes with n≤-8 while the mode with the highest amplitude is typically n=-7 (usually the central one in RFX-mod). This is in agreement with previous observations that showed a low effect on stochasticity of the innermost resonant mode (see Ref. 3 for example).

3. Particle transport

Interaction between the dynamo modes locks them in phase. The locked mode (LM) produces a non axial-symmetric deformation of the last closed magnetic surface (LCMS) [5]. The deformation affects transport introducing non axial-symmetric effects locally modifying both the density profile and the influx from the wall. Due to the plasma wall interaction, density profiles close to the locking position have a steeper edge gradient than at other toroidal positions [14] and particle influx is higher [15]. Controlling the edge radial magnetic field by VS greatly reduces the deformation amplitude [5], but the effect is still present.

Figure 5 shows, as function of the I_p/N parameter, the peaking factor (P) defined as the ratio of the central density to the average density. In figure 5, to avoid LM effect, only density profile measurements far from locking position are considered. The data show that there is no difference on density profiles between RFX and RFX-mod. This is confirmed by performing a multivariable regression of the peaking factor, which gives the scaling $P \propto I_p^{0.14} N^{-0.27}$ (multiple R=0.7) for RFX-mod data and a similar one (with a lower correlation) for RFX. The negative power dependence on density can be explained in terms of neutral particle source that becomes closer to the wall when density increases. The small positive dependence on plasma current is less obvious. It could result from a lower plasma core transport due to a reduced magnetic stochasticity at higher plasma currents.

Although density profiles in RFX-mod VS and in RFX are similar, particle transport is globally reduced in RFX-mod particularly at the highest plasma currents where RFX was strongly affected by LM. This results from the lower particle influx of RFX-mod discharges. In RFX-mod particle influx measured at H_α diagnostic section shows no correlation with the toroidal position of the m=1 helical component of the LM deformation. In discharges with a plasma current higher than 800 kA a small increase of particle influx is present when the toroidal position of the m=0 shrink component of LM deformation is very close to the H_α

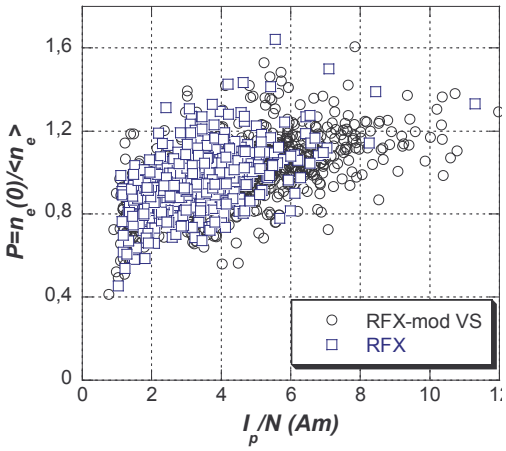

FIG. 5. Density profile peaking for RFX and RFX-mod VS discharges.

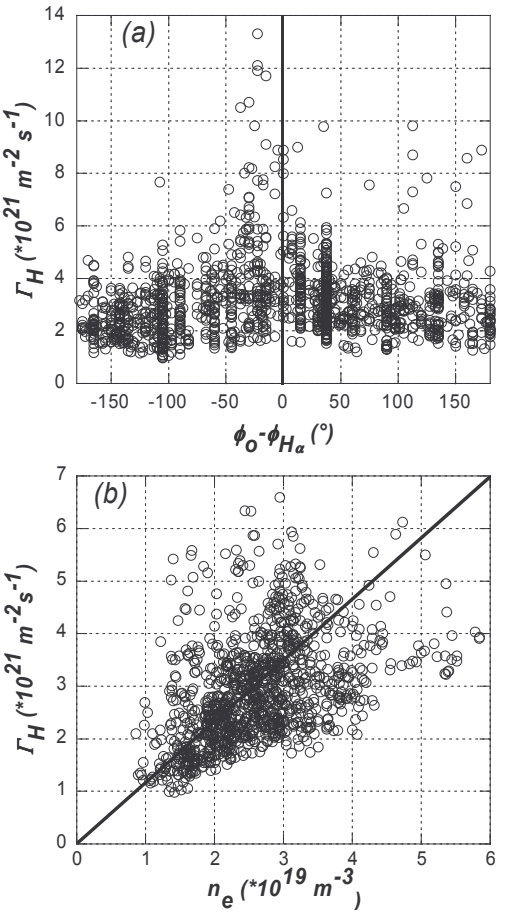

FIG. 6. Particle influx for RFX-mod (VS) discharges with plasma current >800 kA. a) Particle influx versus toroidal distance of the m=0 LCMS shrinking from H_α measurement; b) Particle influx versus average plasma density.

measurement section (FIG. 6a). On average the influx depends linearly from the density with a value of $3\cdot10^{21}$ $m^{-2}s^{-1}$ for a density of $2.5\cdot10^{19}$ m^{-3} (FIG. 6b) which corresponds to a global particle confinement of about 2 ms. In the same plasma current range (>800 kA) on RFX about 40% of particle influx [15] came from a region close to the m=1 LM. Due to the strong wall interaction and the poor particle confinement in RFX the global influx was independent on density with a value $\geq6\cdot10^{21}$ $m^{-2}s^{-1}$ more than two times higher than in RFX-mod VS.

Particle transport is simulated using a 1-D transport code that solves the transport equation. Following the RR theory of diffusion in a stochastic magnetic field [2,16], we include in the convective velocity component of particle flux a velocity proportional to the stochastic coefficient (D_{st}) and the normalised temperature gradient:

$$V_{st} = -\frac{D_{st}(r)\,\partial T(r,t)}{2T(r,t)\quad \partial r}$$

To find D_{st} we parameterise it with five free parameters in the following way:

$$D_{st}(r) = (D_0 - D_{e1})(1-r^{\alpha})^{\beta} + D_{e2}r^{30} + D_{e1}$$

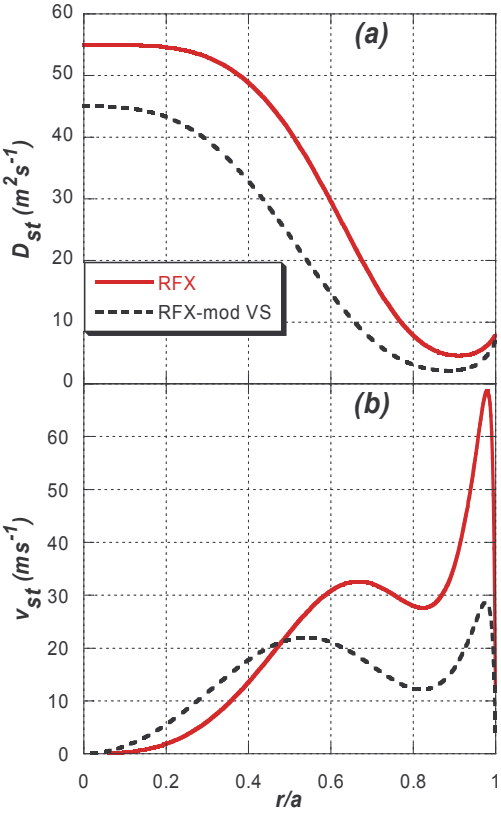

FIG. 7. Diffusion coefficient and stochastic velocity obtained for RFX (red solid curves) and RFX-mod VS (black dashed curves).

The profile of atoms coming from the wall is computed with the Monte Carlo code NENE (NEutrals and NEutrals), based on the work of Hughes and Post [17]. The interaction of the particles with the wall is modelled using the results of the TRIM code (TRansport of Ion in the Mass) [18], a Monte Carlo code for simulation of sputtering, ion reflection and ion implantation in structure-less solids.

We evaluate the D_{st} on RFX and RFX-mod by simulating the same typical density profile at $\langle n_e \rangle = 3\cdot10^{19}$ m^{-3}. For RFX-mod the influx is $\Gamma_H = 3\cdot10^{21}$ $m^{-2}s^{-1}$ and the exponent of temperature profile is $\alpha_T = 3$; for RFX we use $\Gamma_H = 6\cdot10^{21}$ $m^{-2}s^{-1}$ and $\alpha_T = 4$ because flatter temperature profiles were found in RFX. Figure 7 shows the diffusion coefficient and the consequent outward velocity in the two cases. As it can be expected from the halving of the particle influx, the diffusion coefficient of RFX-mod is approximately halved on all the plasma section. Although the errors in D_{st} are large, the result seems to indicate that in RFX-mod the particle confinement improves on the whole section as effect of a simultaneous reduction of the plasma-wall interaction and of the core magnetic stochasticity.

4. Energy transport

Energy transport is greatly improved in RFX-mod VS operations. The maximum of the central electron temperature, T_{eo}, increases nearly linearly with plasma current up to 1 MA while RFX showed electron temperature saturation over 800 kA (see FIG. 8), giving a T_{eo} in RFX-mod VS about 30% higher than in RFX discharges.

Higher core electron temperature indicates a decrease of electron heat transport in RFX-mod VS. An estimate of such a reduction is obtained by applying the 1D steady state power balance equation [19,20]. The effective thermal conductivity, χ_{eff} (FIG. 9), is deduced by using the single fluid equation:

$$\chi_{eff} = -q_{\perp}(r)/[n_e(r)\cdot\nabla T_e(r)]$$

in which the energy flux, $q_{\perp}(r)$, is evaluated by integrating the expression

$$\nabla q_{\perp}(r) = \Omega(r) - \varepsilon(r)$$

where $\Omega(r) = E(r)\cdot j(r)$ is the ohmic power deposition profile and $\varepsilon(r)$ is the experimental total radiation emissivity, mostly localized in the plasma edge and typically ranging from 5% to 20% of the input power. The current density $j(r)$ profile is reconstructed from external magnetic measurements with the μ&p-model [21]. $E(r)$ is modelled through a local Ohm's law with Spitzer resistivity, with an effective charge assumed uniform over the line integral of a line-free visible continuous emission.

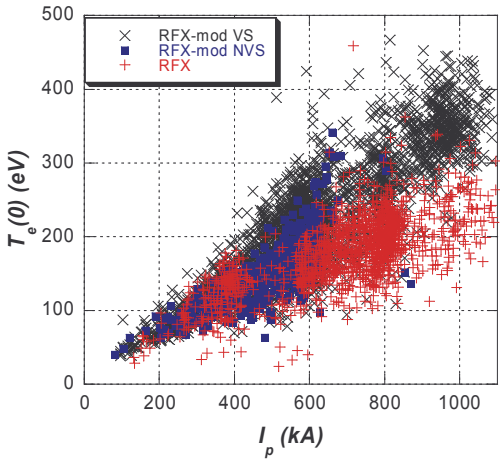

FIG. 8. Central electron temperature dependence from plasma current.

Edge radial field control during VS operations (blue profiles in FIG. 9) decreases the field stochasticity in the core, with the effect of slightly reducing the minimum value of χ_{eff} by about 20%. Interestingly, the main effect is in the inner region, r/a~[0.5-0.7], where the temperature gradient is still appreciably non-zero, and the average χ_{eff} is about 5 times lower than in the NVS operation. Even better performances are obtained in the third case (green profiles in FIG. 9): it is characterised by low amplitude of all modes at the edge and relatively large internal amplitude of the n=-7 mode thus realising a QSH state. This causes an increased electron temperature and the formation of a significant temperature gradient in the core region, shown in FIG. 9. The presence of the helical structure is confirmed by SXR tomography, and predicted by simulations by guide centre codes.

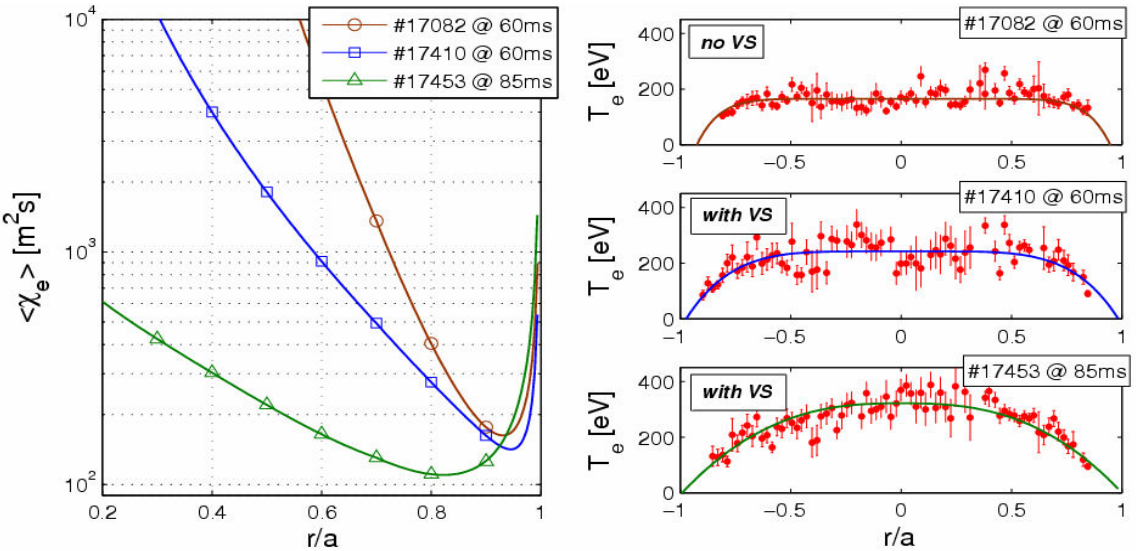

FIG. 9. χ_{eff} and corresponding Te profiles in three representative profiles, in NVS (brown), VS (blue) and an optimum case (green).

5. Conclusions

An analysis of RFX confinement properties in stationary discharges both in terms of global parameters scaling and of local transport was presented in the plasma current range I_p=0.3÷1 MA.
The statistical analysis has shown that the thin shell solution, supplemented by a feedback system to control edge radial field, improves RFP plasma confinement. The control of edge radial field clearly allows to extend operations to high plasma current without suffering any degradation of confinement. This provides high electron temperature and doubles particle and energy confinement times at plasma current of 1 MA compared to the thick shell RFX. A maximum of 3 ms particle confinement time and 1.5 ms energy confinement time was obtained with an applied toroidal field of only 15 mT.
Improved particle transport does not modify density profile, in agreement with a neutral source close to the edge and a reduction of diffusion coefficient on the whole plasma section.
Energy transport analysis shows a reduction of thermal conductivity both in the core and at the plasma edge. Analysis of some of the best discharges revealed that improved confinement in some cases is due to the spontaneous transition to a QSH state associated to low edge error fields.

Acknowledgement: This work was supported by the European Communities under the contract of Association between EURATOM/ENEA.

References

[1] Spizzo G., et al., Phys. Rev. Lett. **96** (2006) 025001.
[2] Rechester A.B. and Rosenbluth M.N., Phys. Rev. Lett. **40** (1978) 38.
[3] Sarf J.S., et al., Nucl. Fusion **43** (2003) 1684.
[4] Paccagnella R., et al., Phys. Rev. Lett. **97** (2006) 075001.
[5] Martini S., et al., Overview of RFX-mod Results with Active MHD Control, This conference, EX/7-3.
[6] Cappello S. and Biskamp D., Nucl. Fusion **36** (1996) 571.
[7] Cappello S. and Paccagnella R., Phys. Fluids B **4** (1992) 611.
[8] Escande D.F., et al., Phys. Rev. Lett. **85** (2000) 1662.
[9] Alfier A., et al., in Proceedings of 33th Conference of the European Physical Society, Rome, (2006) P5.089.
[10] Innocente P. and Martini S., Rev. Sci. Instrum. **63** (1992) 4996.
[11] Gregorato D., et al., Nucl. Fusion **38** (1998) 1199.
[12] Brunsell P. R., et al., IAEA 2000.
[13] D'Angelo F., Paccagnella R., Phys. Plasmas **3** (1996) 2353.
[14] Lorenzini R., et al., in Proceedings of 33th Conference of the European Physical Society, Rome, (2006) P5.082.
[15] Valisa M., et al., J. Nucle. Mater. (2001) 290.
[16] Arvey R.W., et al., Phys. Rev. Lett. **47** (1981) 102.
[17] Hughes M.H. and Post D.E., J. Comput. Phys. **28** (1978) 43.
[18] Biersack J.P. and Haggmark L.G., Nucl. Instr. and Meth. **174** (1980) 257.
[19] Bartiromo R., et al., Phys. Plasmas **6** (1999) 1830.
[20] Pasqualotto R., et al., in Proceedings of 26th EPS Conference on Controlled Fusion and Plasma Physics, Maasrticht, ECA Vol. 23J (1999) 1153.
[21] Ortolani S. and Schnack D.D., *Magnetohydrodynamics of Plasma Relaxations* (World Scientific, Singapore (1993).